Into Eurasia: A geometric morphometric re-assessment of the Upper Cave (Zhoukoudian) specimens

Katerina Harvati [a,b,*]

[a] *Department of Early Prehistory and Quaternary Ecology and Tübingen/Senckenberg Center for Human Evolution and Paleoecology, Eberhard Karls Universität Tübingen, Germany*
[b] *Department of Human Evolution, Max Planck Institute for Evolurionary Anthropology, Germany*

ARTICLE INFO

ABSTRACT

Since the discovery of the human remains from the Upper Cave of Zhoukoudian in the 1930s there has been speculation over their affinities. In particular, the degree to which the three adult crania exhibit recent East Asian morphology, as well as their degree of within-group variability, has long been debated. Several early researchers described a resemblance to East Asian populations, but these findings have been for the most part rejected by more recent metric and non-metric analyses. Nevertheless, the Upper Cave specimens have not been classified conclusively into any recent modern human population to which they have been compared, and classification results differ for each cranium. Here, the question of the affinities of Upper Cave 101 and 103, the two better-preserved crania, is examined from the perspective of the Late Pleistocene human fossil record using the methodology of 3-D geometric morphometrics. The degree of morphological variation between the two specimens is also evaluated within the context of recent population variability. Neurocranial and facial morphology are analyzed separately so as to maximize comparative samples. Results show a morphological resemblance of the Upper Cave material to Upper Paleolithic Europeans. It is proposed that the Upper Cave specimens retain important aspects of modern human ancestral morphology, and possibly share a recent common ancestral population with Upper Paleolithic Europeans, in accordance with the Single Origin model of modern human origins.

© 2009 Elsevier Ltd. All rights reserved.

Introduction

The specimens from the Upper Cave (Shandingdong), Zhoukoudian, are thought to be among the earliest representatives of modern humans in Asia. Since their discovery in the early 1930s there has been discussion over their affinities, and their possible links with recent Asian people and with more ancient Asian fossils have been debated (e.g., Thorne and Wolpoff, 1992; Stringer, 1992a; Wright, 1992, 1995; Wolpoff, 1995). These specimens were originally assumed to be of great antiquity and penecontemporaneous with European Upper Paleolithic humans (Weidenreich, 1938–39). However, their chronology has not been conclusively resolved and uncertainties remain about the stratigraphic integrity of the site and the provenience of some of the material (see Kamminga, 1992; Brown, 1999). Early conventional radiocarbon dates on faunal bone samples indicated a radiocarbon age of $10,175 \pm 360$ years B.P. for the

human occupation layer, and $18,340 \pm 410$ years B.P. for the deeper layers, suggesting a Terminal Pleistocene or Holocene age for the human remains (Wu and Wang, 1985; Brown, 1993). More recent AMS radiocarbon dates, again on faunal bone, range from $13,200 \pm 160$ years B.P. to $33,200 \pm 2000$ years B.P., with a proposed radiocarbon date of 24–29 ka for the cultural layers, supporting the original assessment of an Upper Paleolithic chronology for the human remains (Chen et al., 1989; Hedges et al., 1992; Brown, 1993).

Although the Upper Cave (UC) specimens are clearly modern in their cranial morphology, determining their regional affinities has proven difficult. Results vary among studies and for each of the three crania. In his first report on the specimens, Weidenreich (1938–39) saw similarities with the European Upper Paleolithic material in the cranial and facial morphology of the older, presumed male specimen UC 101. He considered this individual, dubbed the "Old Man," as more archaic than even some of the "Cro-Magnons" in its low cranial vault and heavy browridges. Nonetheless, he also saw subtle similarities to East Asians in some of its facial features. Weidenreich considered the UC 102 and 103 crania, both presumed females, to be of "Melanesian" and "Eskimoid" affinities, respectively. He concluded that the Upper Cave group was a highly heterogeneous "proto-Mongoloid" population, and not particularly similar to later East Asian groups.

* Corresponding author. Department of Early Prehistory and Quaternary Ecology, Zentrum für Naturwissenschaftliche Archäologie Rümelinstr. 23, 72070 Tübingen, Germany.
E-mail address: katerina.harvati@ifu.uni-tuebingen.de

Subsequent treatments of this subject using morphological descriptions and univariate analyses of cranial linear measurements or indices found East Asian or archaic East Asian affinities, especially in the face (Wu, 1960, 1961; Coon, 1962; Wolpoff, 1996), supporting regional Asian continuity in modern human evolution. To these studies must be added the assessment of the dental pattern shown by the Upper Cave individuals, which has been evaluated as sinodont, and therefore East Asian, in character (Turner, 1985; Turner et al., 2000), though the accuracy of scoring dental traits on the existing casts of the Upper Cave specimens has been questioned (Brown, 1999).

In more recent years, several analyses demonstrated the nonregional character of several presumed "East Asian" non-metric traits often used to support regional continuity in this region (e.g., Bräuer, 1989; Groves, 1989; Habgood, 1989; Bräuer and Mbua, 1992; Lahr, 1994, 1996; Lieberman, 1995), putting some of these earlier results into question. The most recent assessment of the Upper Cave non-metric morphology (Liu et al., 2006) used twelve East Asian non-metric traits and showed that the three most complete crania (UC 101, 102, and 103) differ from Holocene East Asians in the expression of eight of these features. The Upper Cave crania showed an elevated robusticity in seven of these traits (sagittal keel, occipital torus, supraorbital torus, nasal saddle, infraglabellar notch, zygomaxillary tuberosity, and zygomatic trigone), while one (lambdoid flattening) was less pronounced in Upper Cave than it was in Holocene Chinese groups. The authors interpreted these differences as either retentions of morphology that is primitive (in the cladistic sense) in relation to Holocene humans or (in the case of the nasal bridge morphology) as possibly reflecting adaptation to the climatic conditions of the Final Pleistocene (Liu et al., 2006).

In contrast to earlier descriptions and univariate analyses, most morphometric analyses of the Upper Cave material have found no similarities between these crania and recent East Asians. Rather, they have variably classified the Upper Cave remains with Australo-Melanesians, Africans, Polynesians, and ancient American populations (Howells, 1983, 1989, 1992; Habgood, 1986; Kamminga and Wright, 1988; Kamminga, 1992; Stringer, 1992a; Wright, 1992, 1995; Lahr, 1995; Neves and Pucciarelli, 1998; Brown, 1998, 1999; Cunningham and Jantz, 2003). Despite these efforts of classification, these specimens are not typical (using the measure of typicality probability) of any population to which they are compared (Cunningham and Jantz, 2003). Moreover, in keeping with Weidenreich's original assessments, the Upper Cave crania seem to show greater variability than would be expected for recent populations, suggesting that a high level of heterogeneity might generally characterize Late Pleistocene modern human groups (Cunningham and Wescott, 2002). Several of these studies have suggested some degree of retention of ancient *Homo sapiens* morphology by the UC specimens and a resemblance to early modern human populations, such as early Australians, Paleoamericans, and archaic Native Americans (e.g., Habgood, 1986; Stringer, 1992a; Hanihara, 1994; Neves and Pucciarelli, 1998; Brown, 1999; Cunningham and Jantz, 2003).

Despite suggestions of retention of morphology considered primitive relative to Holocene humans, and perhaps because of the uncertainty surrounding the specimens' geological age, their affinities with Upper Paleolithic Europeans have not been examined in depth. With few exceptions, most previous research has been restricted to comparisons with recent humans and has included few, if any, Late Pleistocene human fossils. Habgood (1986) conducted a multivariate analysis of 24 linear cranial measurements of the three Upper Cave crania as part of a restricted sample of early modern Asian, Australian, European, and African fossil specimens. He detected resemblances between UC 101 and the Wadjak individuals, UC 102 and the Southwest Asian specimen

Hotu 2, and between UC 103 and Liujian. Although it suggested a degree of similarity among these early modern humans, that study did not take into account recent modern human variation, and thus could not fully evaluate the morphological affinities of the Upper Cave crania. Stringer (1992a) conducted a multivariate analysis on 38 linear cranial measurements taken on a sample of early modern humans from the Levant, Europe, and Australia, recent humans from Africa, Europe, Australia, and North America, as well as Neanderthals and Middle Pleistocene fossil humans. In his analyses the Upper Cave specimens did not resemble modern Asians, but instead grouped with recent Australians and Africans. They also showed a degree of similarity to the early modern human samples (Stringer, 1992a). Both Habgood (1986) and Stringer (1992a) found different regional affiliations for each of the Upper Cave crania analyzed, in keeping with previous interpretations of elevated levels of heterogeneity in this skeletal sample.

The present study aims to re-evaluate both the morphological affinities and level of within-group variation of the Upper Cave individuals using 3-D geometric morphometrics. These methods have not been used to analyze this material to date, but they have some advantages relative to traditional morphometric techniques (see below) and may thus provide additional insights to previous research. Furthermore, following Stringer (1992a), the present analysis focuses not only on regional recent human variation, but also on the later Pleistocene human fossil record from the Old World, taking into account recent developments in the assessment of the geological date of fossil specimens (see Trinkaus, 2005). The two better-preserved crania from the Zhoukoudian Upper Cave locality, UC 101 and UC 103, were analyzed using a comparative sample of modern humans from a wide geographic range, early modern humans and Middle-Late Pleistocene fossils from Eurasia and Africa. If the UC individuals were already on the differentiated lineage of recent East Asians, they would be expected to show distinct morphological similarities with the East Asian modern human sample. Alternatively, if the UC specimens largely retain morphology ancestral for recent *H. sapiens*, they would be expected to show morphological affinities to early modern human fossils such as the European Upper Paleolithic material or even the earlier anatomically modern specimens.

Materials and methods

Samples included several Pleistocene human fossil specimens from Asia, Europe, Africa, and the Near East, and two hundred and eighty-four recent human crania representing seven broad geographic groups (Tables 1 and 2).

Only adults were included, as determined by fully erupted permanent dentition. The sex of the modern human crania was assigned on the basis of museum catalog records, cranial morphology and size, and, in the rare cases of associated postcrania, pelvic morphology. Inasmuch as possible, male and female samples were balanced for sample sizes. Since such sex assignment is imperfect for recent humans, and even more problematic for fossil specimens, sexes were pooled in the analyses, with the exception of the inter-individual Procrustes distances analysis.

In the few cases where original fossil specimens were not available, high quality casts or stereolithographs from the collections of the Division of Anthropology of the American Museum of Natural History, the Department of Anthropology at New York University, the Institut de Paléontologie Humaine, and the Department of Human Evolution at the Max Planck Institute for Evolutionary Anthropology were measured. Using casts as alternatives to fossil specimens is an imperfect solution, and recently it has been pointed out that this practice may introduce substantial error (McNulty and Smith, 2009). Nevertheless, substituting casts for original specimens is necessary in cases where the originals are

Table 1
Fossil comparative samples used in the analysis.

European and West Asian H. neanderthalensis (n = 12; NEA)

Amud 1 (Am1)
Feldhofer 1[a] (Fh1)
Gibraltar 1 (Gb1)
Guattari (Gt)
La Chapelle-aux-Saints (Ch)
La Ferrassie 1 (Fr1)
La Quina 5 (Qn)
Shanidar 1,[a] Shanidar 5[a] (Sh1, Sh5)
Spy 1, Spy 2 (Sp1, Sp2)
Tabun 1 (Tb1)

Middle Pleistocene Europeans (n = 3; MPE)
Arago[a] (Ar)
Petralona (Pe)
Sima de los Huesos 5[a] (Sm5)

Middle Pleistocene Africans (n = 3; MPA)
Bodo (Bd)
Kabwe (Kb)
Saldanha (Sl)

Middle Pleistocene East Asians (n = 1; DAL)
Dali[a] (Da)

Late Middle-Late Pleistocene fossils from Africa and the Levant (n = 7; LPA, EAM)
Irhoud 1, Irhoud 2 (Ir1, Ir2)
Ngaloba (LH18)
Qafzeh 6,[a] Qafzeh 9 (Qz6, Qz9)
Singa (S1)
Skhul 5 (Sk5)

Upper Paleolithic Eurasian modern humans (n = 19; EUP, LUP)
Upper Cave 101,[a] 103[a] (UC101, UC103)
Abri Pataud (AP)
Cioclovina (Ci)
Chancelade (Cn)
Cro Magnon 1, 2, 3 (CM1, CM2, CM3)
Grimaldi 4[a] (Gr)
Mladeč 1, 5 (Ml1, Ml5)
Předmostí 3,[a] 4[a] (Pd3, Pd4)
Dolní Věstonice 3, 13, 15, 16 (Dv3, Dv13, Dv15, Dv16)
Brno 1 (Bn1)
Ohalo II[a] (Oh2)

The symbols for each specimen used in Figs. 2 and 3 are indicated in parentheses.
[a] Indicates specimens for which high-quality casts or stereolithographs were measured.

Table 2
Recent human comparative samples employed. The population labels used in Figs. 1 and 2, the geographic and temporal provenience of the samples, and the museums where they are curated are indicated in parentheses and footnotes. Symbols as follows: m = males, f = females, u = unknown sex.

Recent human samples	Face	Vault
African (AFR; Kenya, Zulu; sub-recent; NHM, WITS)	m = 17	m = 15
	f = 13	f = 12
Andamanese (AND; Andaman Islands; sub-recent; NHM)	m = 14	m = 14
	f = 15	f = 14
Asian (AS; China, Thailand; sub-recent; MH)	m = 20	m = 19
	f = 18	f = 18
		u = 2
Oceanic (OCE; Australia, Torres Islands, Tasmania; sub-recent; NHM)	m = 16	m = 21
	f = 10	f = 13
		u = 8
Khoesan (KH; South Africa; Holocene[a]; IZCT, UCT)	m = 35	m = 37
	f = 16	f = 19
	u = 4	u = 3
New World (NW; Alaska, Greenland, Utah; sub-recent; AMNH)	m = 18	m = 17
	f = 14	f = 15
	u = 2	u = 2
West Eurasia (WE; Europe, Syria; sub-recent; IAL, MH)	m = 21	m = 21
	f = 14	f = 14
Total	**n = 247**	**n = 264**

Museum abbreviations: AMNH: American Museum of Natural History, New York; IAL: Institute of Anatomy, Leipzig; IZCT: Iziko Museums of Cape Town; MH: Musée de l'Homme, Paris; NHM: Natural History Museum, London; UCT: University of Cape Town; WITS: University of the Witswaterand, Johannesburg.
[a] Stynder et al., 2007.

not available and particularly where the originals no longer exist, as is the case with the Upper Cave remains or with the Předmostí Upper Paleolithic fossils.

For the purposes of the Mahalanobis D^2 and mean Procrustes distance analyses (see below), the fossil samples were partitioned in the following groups: *H. neanderthalensis* (NEA); Middle Pleistocene Europeans (MPE); Middle Pleistocene Africans (MPA); Dali (DAL); Early anatomically modern humans from Qafzeh and Skhul (EAM); Late Pleistocene Africans (LPA); Early Upper Paleolithic Europeans (EUP; comprising Cioclovina, Mladeč 1 and 5); Late Upper Paleolithic Europeans (LUP); and Zhoukoudian Upper Cave 101 and 103 (UC).

Data were collected in the form of three-dimensional coordinates of facial and neurocranial osteometric landmarks, defined as homologous points that can be reliably and repeatedly located, using a Microscribe (Immersion Corp., 1998) portable digitizer (Table 3). Additionally, landmarks along the midsagittal profile from glabella to inion, along the coronal and lambdoid sutures, and along the upper margin of the supraorbital torus were also registered (Table 3). The points along these outlines were automatically resampled to yield the same semilandmark count on every specimen (Bookstein, 1997; see also Gunz and Harvati, 2007). Points were chosen so as to reflect the facial and neurocranial morphology

of the fossils as fully as possible. Because of the differential preservation of the comparative fossil sample, two datasets were prepared: a facial landmarks dataset and a neurocranial landmark and semilandmark dataset.

The data were processed using geometric morphometric methods (GMM). These methods provide some advantages to traditional morphometric analyses. They preserve the geometry of the object studied better than traditional measurements, and thus allow for a better analysis of shape; readily account for size correction; enable the identification of landmarks where shape differences occur and the relative levels of difference at each landmark; enable visualization of the shape changes between specimens in specimen space; and, perhaps most importantly, enable the quantification of some traits that are difficult to measure with conventional measurements (Rohlf and Marcus, 1993; O'Higgins, 2000). Because of these qualities, GMM have gained widespread and increasing use in the recent literature on human variation (e.g., Harvati, 2003; Stynder et al., 2007; González-José et al., 2008; Smith, 2009). Despite these general advantages of GMM, it does not accommodate missing data, often necessitating some level of data reconstruction in fossil studies. Therefore, landmarks on specimens with minimal damage were estimated during data collection using anatomical clues from the preserved surrounding areas. Bilateral landmarks and curves missing on one side were further reconstructed by superimposing the landmark configurations of specimens with missing data with their reflections, and by substituting the coordinates for each missing landmark with the fitted homologous counterpart on the other side. This is a process known as "reflected relabeling" (see Mardia and Bookstein, 2000). For the distorted specimen Arago 21, a reconstruction based on reflected relabeling (Gunz, 2005; Gunz et al., 2009) was used. Further data reconstruction was allowed in the case of LH 18, an important specimen with only minimal damage (frontomalare temporale is missing on both sides). Semilandmarks were "slid" in Mathematica (Wolfram Research, Inc., 2007) using routines developed by Philipp Gunz and Philipp Mitteroecker (Gunz et al., 2005; for additional details on semilandmark processing and data reconstruction see Gunz and Harvati, 2007; Harvati et al., 2007). Landmarks and slid semilandmarks were superimposed with

Table 3
Landmarks and semilandmarks used in the analysis.

FACE LANDMARKS	
1. Glabella (GLA)	
2. Post-toral Sulcus	Minima of concavity on midline post-toral frontal squama
3, 4. Mid-orbit Torus Superior	Right and Left
	Point on superior aspect of supraorbital torus, approximately at the middle of the orbit
5, 6. Mid-orbit Torus Inferior	Right and Left
	Point on inferior margin of supraorbital torus, approximately at the middle of the orbit
7. Nasion	
8, 9. Dacryon	Right and Left
10, 11. Alare	Right and Left
12, 13. Zygoorbitale	Right and Left
14, 15. Zygomaxillare	Right and Left
16, 17. Infraorbital foramen	Right and Left
18, 19. Frontomalare Orbitale	Right and Left
20. Nasospinale	
21. Prosthion	
VAULT LANDMARKS	
1. Glabella (GLA)	
2. Post-toral Sulcus	Minima of concavity on midline post-toral frontal squama
3. Bregma	
4. Lambda (LBD)	
5. Inion (IN)	
6, 7. Mid-orbit Torus Superior	Right and Left
	Point on superior aspect of supraorbital torus, approximately at the middle of the orbit
8, 9. Mid-orbit Torus Inferior	Right and Left
	Point on inferior margin of supraobrital torus, approximately at the middle of the orbit
10, 11. Frontomalare Orbitale (FMO)	Right and Left
12, 13. Frontomalare Temporale (FMT)	Right and Left
14, 15. Anterior Pterion (PTE)	Right and Left
16, 17. Parietal Notch	Right and Left
18, 19. Asterion (AST)	Right and Left
VAULT RIDGE CURVES	
1. Supraorbital torus	21 semilandmarks from FMT Right to FMT Left
2. Midsagittal profile	26 semilandmarks from GLA to IN
3. Coronal suture	20 semilandmarks from PTE Right to PTE Left
4. Lambdoid suture	14 semilandmarks from AST right to LBD to AST Left

Table 4
Mean, standard deviation, and range of centroid size for each group, and centroid size values for UC 101 and UC 103. A: Vault, B: Face.

A:

	Mean	St. Dev	Max	Min
MPLA	83.91	1	84.62	83.19
MPLE	79.38	5.31	83.13	75.62
DAL	83.24	–	–	–
NEA	82.9	2.97	86.39	77.08
LPA	82.72	1.02	84.18	81.49
EAM	82.53	0.85	83.4	81.85
AND	72.78	2.8	78.86	69
AS	77	2.99	82.82	72.06
OCE	78.2	3	83.63	71.23
AFR	80.55	2.62	87.55	75.73
NW	78.51	2.41	83.42	73.45
KH	79.15	2.35	84.1	73.16
WE	79.35	3.03	84.72	72.26
EUP	84.47	3.44	87.53	80.74
LUP	83.91	2.82	87.95	78.73
UC101	85.15			
UC103	79.57			

B:

	Mean	St. Dev	Max	Min
MPLA	23.61	1.19	24.45	22.76
MPLE	21.99	1.34	23.54	21.17
NEA	21.29	0.80	22.56	20.32
LPA	20.92	–	–	–
EAM	19.79	0.49	20.14	19.44
AND	16.73	0.49	17.97	15.96
AS	17.79	0.67	19.13	16.16
OCE	17.42	0.60	18.66	16.16
AFR	17.93	0.60	19.18	16.61
NW	18.25	0.72	20.12	16.80
KH	17.22	0.71	18.85	15.62
WE	17.92	0.90	19.87	15.74
EUP	18.17	–	–	–
LUP	18.12	0.80	19.42	17.19
UC101	19.64			
UC103	18.31			

Generalized Procrustes Analysis (GPA) using the Morpheus software package (Slice, 1998). This procedure translates the landmark configurations to common origin, scales them to unit centroid size (the square root of the sum of squared distances of all landmarks to the centroid of the object; the measure of size used here), and rotates them according to a best-fit criterion. GPA thus removes centroid size so that shape can be analyzed separately, although size-related, allometric shape differences may remain.

Superimposed coordinates were analyzed statistically using principal components analysis (PCA), Procrustes distances, and Mahalanobis squared distances. These statistics were calculated with the software packages SAS (SAS Institute, 1999–2001), NTSys (Applied Biostatistics Inc., 1986–2000), and TPSsmall (version 1.20; Rohlf, 2003). The pattern of variation in the sample was evaluated through the PCA, and the similarities among specimens were assessed using inter-individual Procrustes distances (defined as the square root of the sum of squared distances between two superimposed landmark configurations). The latter were plotted directly in the PCA graphs in the form of a minimum spanning tree (MST), a graph that links up all specimens of the dataset with the smallest sum of distances. This graph is independent from the principal components plotted, and reflects overall shape similarity rather than position along the two plotted axes. Inter-individual Procrustes distances were also used to evaluate the degree of heterogeneity of the UC sample relative to the spread of such distances within regional comparative samples.

Similarities among groups were evaluated using Mahalanobis D^2 and mean Procrustes distances between groups. The Mahalanobis statistic represents the morphological difference among groups, scaled by the inverse of the pooled within-group covariance matrix. The larger the values of the D^2 distance, the farther the group centroids are from each other. Mahalanobis D^2 assumes equality of covariance, and therefore might be affected by violations of this assumption (though see Harvati et al. [2005] for a discussion of this issue). Procrustes distance, on the other hand, does not account for non-independence of landmark coordinates and within-group variation. It reflects differences in total shape, and does not take into account patterns of covariation, and, therefore, is not affected by the assumption of equality of covariance. The first 15 principal components (all components accounting for $>0.1\%$ of the total variance following Kaiser [1961]; taken together, they explain approximately 80% of the variance) were used as variables in the Mahalanobis analyses in order to reduce the number of variables. Because sample sizes were not equal, a correction in calculating this statistic was used, following Marcus (1993). Both Mahalanobis squared distances and Procrustes
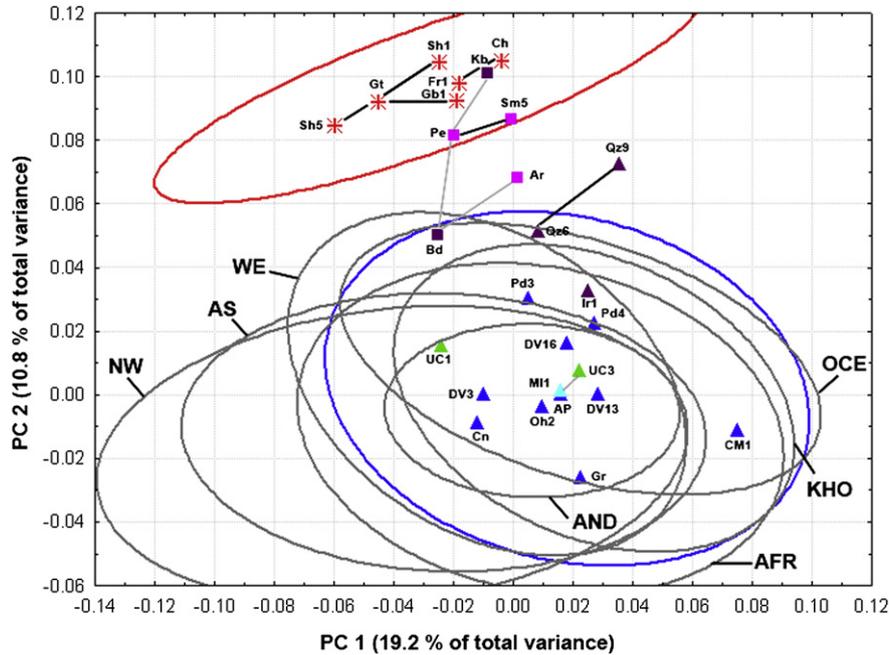
Fig. 1. Principal Components Analysis, vault dataset: PC 1 vs. PC 2, with Minimum Spanning Tree (MST) calculated from Procrustes distances superimposed (connections among fossils from the same group are shown in black; connections among fossils from different groups are shown in gray; for the purpose of clarity, connections among and with recent human specimens are not shown). The MST is based on all dimensions of shape space, not only the two principal components shown here, and thus allows one to check for projection artifacts. NEA: red stars; MPE: pink squares; MPA: purple squares; DAL: open pink square; EAM and LPA: purple triangles; EUP: light blue triangles; LUP: dark blue triangles; UC: green triangles. Ellipses represent 95% confidence ellipses around the modern human populations (gray ellipses, labeled by population), and the Upper Paleolithic (blue ellipse) and Neanderthal samples (red ellipse). Individual fossils and recent population means labeled as in Tables 1 and 2.

distances among mean sample configurations were plotted in Neighbor Joining Trees.

Results

Centroid size

Neurocranial centroid size values are reported in Table 4A. Upper Cave 101 shows a rather large neurocranium, falling at the extreme end of recent human variation. One recent African individual exceeds its value, but it falls well within the range of both Early and Later Upper Paleolithic specimens. It is significantly larger than the Oceanic and Asian samples. The neurocranium of UC 103 is smaller, and more similar in size to the average of several recent human groups, as well as to the smaller Upper Paleolithic specimens. It is not significantly different from any of the samples used.

Upper Cave 101 is again at the high end of the recent human variation in facial size. It is significantly smaller than the largest-sized fossil sample, the African Middle Pleistocene specimens, and significantly larger than the smallest-sized recent human groups, the Khoesan and Andamanese. UC 103 is also smaller than UC 101 in its face, and similar to the mean of some recent populations. It is significantly smaller than the large-sized fossil samples (both African and European Middle Pleistocene fossils, Neanderthals, and Irhoud 1), but not different from any of the recent human groups. Values for the facial centroid size are reported in Table 4B.

Principal components analysis

In the analysis of the vault dataset, the first principal component (PC 1) accounts for 30.9% of the total variance and separates archaic

humans from all modern humans (Fig. 1). This axis reflects differences in vault shape between the fossil and recent humans. On the negative end of PC 1, specimens are characterized by a low and elongated cranial vault, a continuous, supero–inferiorly thick and anteriorly projecting supraorbital torus, and a wide cranial base. Modern human-like scores on the positive end of PC 1 reflect a high, rounded, and antero–posteriorly short cranial vault, supra-orbital ridges whose lateral parts are neither supero–inferiorly thick nor anteriorly projecting (though the glabellar part may be more pronounced), and a narrow cranial base. Upper Cave 101 falls just outside the modern human range on PC 1 as represented by the present samples. It overlaps with early anatomically modern humans from Africa and the Near East, and, like the latter, falls in the outskirts of the Neanderthal 95% confidence ellipse. On the other hand, UC 103 falls well within the modern human range, and very near the Upper Paleolithic specimens Mladeč 1, Cioclovina, and Abri Pataud 1, along this axis. PC 1 is significantly negatively correlated with centroid size but with a low correlation coefficient ($r = -0.23$; $p < 0.0001$).

The second principal component (PC 2) accounts for 10.7% of the total variance and roughly separates the sub-Saharan African, Khoesan, Oceanic, and New World samples (centering on the negative end of PC 2 and characterized by narrower and longer crania) from the Western Eurasian, East Asian, and Andaman ones (centering on the positive end of the axis [Fig. 2] and showing wider and antero–posteriorly shorter crania). However, there is much overlap along this axis among recent human groups. This component shows a stronger negative correlation with centroid size ($r = -0.40$, $p < 0.0001$). Along PC 2, the Late Pleistocene Africans and early anatomically modern humans from the Levant span the entire range of the recent human variation, but the early and later

Fig. 2. Principal Components Analysis, face dataset: PC 1 vs. PC 2, with MST calculated from Procrustes distances superimposed. Symbols and colors are the same as in Fig. 2 and Tables 1 and 2.

Upper Paleolithic samples are for the most part restricted to the negative side of the axis (with the exception of Ohalo 2), with the three EUP specimens falling close to 0. Upper Cave 101 and 103 are also quite central on this axis, falling near the early Upper Paleolithic specimens, Skhul 5 and Qafzeh 9.

For the facial dataset, PC 1 (19.2% of the total variance; Fig. 2) captures differences between the New World sample, particularly the Inuit material (supero–inferiorly tall, flat faces with anteriorly rotated zygomatics) and the remaining recent human groups (supero–inferiorly shorter faces, with more pronounced alveolar prognathism). The New World, Asian, and Western Eurasian samples fall on the negative side, while the Khoesan, sub-Saharan African, Oceanic, and Andaman samples fall on the positive side of this axis. The only early Upper Paleolithic specimen included in the facial analysis, Mladeč 1, as well as most other Upper Paleolithic specimens, are relatively central along this axis (with the exception of Cro Magnon 1, which fell on the extreme positive end of PC 1). Both UC specimens fall well within the 95% confidence ellipse of the Upper Paleolithic sample, though they are located in the region of overlap of all modern human regional groups. This component is significantly negatively correlated with centroid size but with a relatively small correlation coefficient ($r = -0.25$, $p > 0.0001$).

The second principal component (10.8% of the total variance) separates archaic humans from modern human specimens. Archaic specimens score high on PC 2, which reflects supero–inferiorly tall, anteriorly projecting faces, retreating frontal squama, heavy browridges with projecting glabella, and narrow, sagittally rotated zygomatic regions. Modern specimens score low on this axis, reflecting supero–inferiorly short faces, with light browridges and a flatter glabella, steeply rising frontal squama, and broader, coronally rotated zygomatics. Both Upper Cave specimens fall well within the range of modern human variation along this axis, showing similar scores to most Upper Paleolithic Europeans. Again, PC 2 is negatively correlated with centroid size ($r = -0.53$, $p = 0.016$), reflecting the large size of the face in the archaic sample.

Similarity among individuals

Procrustes distances among individual specimens were calculated and used in building minimum spanning trees (superimposed directly on the PCA plots in Figs. 1 and 2). The vault dataset includes a relatively large sample of Upper Paleolithic specimens, and they are often linked to each other in the MST. Such links are observed between Cro Magnon 1 and Předmostí 3, Abri Pataud 1, Cioclovina, and Mladeč 1, and between Cro Magnon 3 and Předmostí 4 (Fig. 2). UC 101 is joined to Předmostí 3 in the Procrustes distance MST, and UC 103 to a New World specimen (Utah 15). The face dataset includes a smaller sample of Upper Paleolithic specimens, and only one early Upper Paleolithic individual, Mladeč 1. This specimen is linked in the Procrustes distance MST to UC 103 (Fig. 3). UC 101 is linked to an Oceanic specimen (Australian 26).

Inter-individual Procrustes distances were also used to evaluate the level of heterogeneity between UC 101 and 103 relative to the morphological variability of the recent human samples. Most modern human samples used here are regional in character, and do not represent demes. However, the Andaman sample is restricted geographically and derives from a homogeneous, isolated island population. It therefore might be most relevant when assessing the level of inter-individual variability among the UC specimens. Since UC 101 is presumed to be male and UC 103 female, the distances between same-sex specimens were excluded. Table 5 presents the mean, range, and 95th percentile of the male–female inter-individual Procrustes distances for each recent modern human reference sample for the vault and facial data, compared to the Procrustes distances between UC 101 and UC 103 for the two datasets. This analysis reveals that the two UC specimens differ more in their vault morphology than they do in the face: their vault Procrustes distance is quite elevated compared to the variability observed in the recent samples. However, it is within the 95th percentile of inter-individual Procrustes distances of all recent regional samples, and just over the 95th percentile (but still within the range) of the Andamanese sample. The face Procrustes distance between UC 101 and UC 103
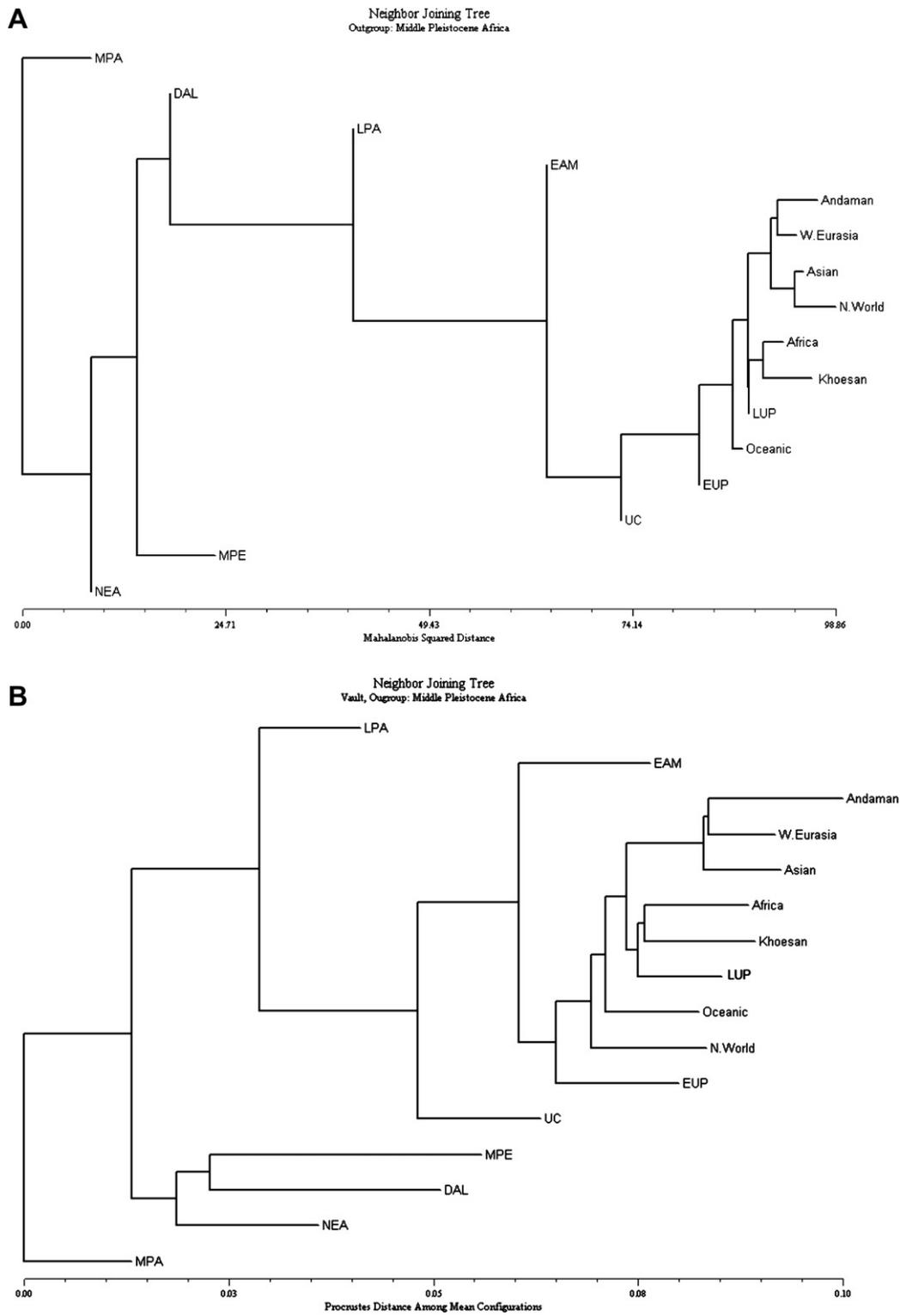
Fig. 3. Neighbor Joining Tree, vault dataset. A: Mahalanobis squared distances; B: Procrustes distances among mean sample configurations. Labels are the same as in Tables 1 and 2.

is much lower, and more similar to the average values observed in all recent human reference samples.

Similarity among groups

Mahalanobis squared distances among samples and Procrustes distances among mean sample configurations were also calculated

and are reported in Table 6. The first 15 principal components were used as variables in calculating the Mahalanobis D^2, accounting for 82.1% and 81.7% of the total variance for the vault and face analyses, respectively. Both distance measures showed similar patterns, with the Upper Cave specimens being more similar to early modern human samples than to recent human groups or to archaic human samples. In the vault, the combined UC sample is relatively far from

Table 5
Mean, maximum, minimum and 95th percentile of the male–female inter-individual Procrustes distances for the recent human population samples compared to the Procrustes distance between UC 101 and UC 103.

	Mean	Max	Min	95th Percentile
UC101–UC103	**0.075**			
Male–female inter-individual Procrustes distances–Vault				
African	0.059	0.091	0.036	0.081
Khoesan	0.059	0.106	0.032	0.081
Andaman	0.055	0.078	0.035	0.072
Asian	0.068	0.108	0.033	0.093
Oceanic	0.058	0.095	0.035	0.077
New World	0.061	0.104	0.037	0.084
West Eurasian	0.064	0.108	0.037	0.086
UC101–UC103	**0.092**			
Male–female inter-individual Procrustes distances–Face				
African	0.104	0.153	0.06	0.135
Khoesan	0.101	0.165	0.057	0.131
New World	0.100	0.176	0.058	0.139
Oceanic	0.104	0.153	0.066	0.132
Asian	0.102	0.205	0.062	0.150
Andaman	0.081	0.114	0.053	0.100
West Eurasian	0.101	0.144	0.062	0.129

most recent human groups, including the Asian sample. It is closest to early modern humans: the Skhul-Qafzeh, early European Upper Paleolithic, and to a lesser extent, the late European Upper Paleolithic and the recent Oceanic samples. The UC sample was also quite distant from the earlier fossil samples. Among these, it was closest to the LPA and rather distant from Dali (though closer to this specimen than to the Middle Pleistocene Africans and Europeans and to the Neanderthal samples). Dali, in turn, shared closest

similarities with the European Middle Pleistocene individuals. In the face, the UC sample is again quite distant from most recent human samples, and not particularly close to the Asian modern humans. It is closest to the late European Upper Paleolithic and to the recent Oceanic sample.

The Neighbor Joining Trees (NJT; Figs. 3 and 4) are very similar for both distance measures and across anatomical datasets. Both the Mahalanobis and Procrustes NJTs from the vault analysis (Fig. 3A,B) and the NJT for the facial Mahalanobis distances (Fig. 4B) show the UC sample as an outgroup to recent human variation, not grouping with any recent human sample. The facial mean Procrustes distance NJT (Fig. 4B) shows a slightly different pattern, with UC grouping with the Oceanic sample in the first branch of the recent human cluster.

Discussion

The analysis of the 3-D shape of the Upper Cave 101 and 103 neurocranial and facial data suggests that these two specimens share morphological similarities with Upper Paleolithic Europeans, as well as with other early anatomically modern humans from the Levant and Africa, indicating retention of early modern human morphology in these specimens. The results of the principal components analyses, inter-individual Procrustes distances in the vault (for UC 101) and the face (for UC 103), the Mahalanobis D^2 and mean Procrustes distances and cluster (Neighbor Joining Tree) analyses for both datasets support such a connection. Particularly striking is the finding that, out of a large sample of modern human specimens, UC 101 was closest neighbor in the shape of its vault (as measured by Procrustes distance) to

Table 6
Mahalanobis D^2 and Procrustes distances among mean configurations. A: Vault. B: Face. Mahalanobis D^2 values corrected for unequal sample size (Marcus, 1993).

A

	MPA	DAL	MPE	LPA	NEA	EAM	AND	AS	OCE	EUP	AFR	NW	KH	UC	LUP	WE
MPA	—	0.056	0.075	0.056	0.054	0.089	0.123	0.116	0.093	0.087	0.107	0.099	0.108	**0.078**	0.101	0.113
DAL	12.33	—	0.064	0.069	0.050	0.105	0.135	0.128	0.109	0.098	0.119	0.109	0.122	**0.090**	0.116	0.124
MPE	26.30	5.11	—	0.076	0.058	0.103	0.132	0.128	0.112	0.108	0.125	0.114	0.130	**0.092**	0.124	0.125
LPA	22.84	16.39	28.41	—	0.052	0.060	0.090	0.083	0.067	0.055	0.079	0.067	0.076	**0.050**	0.070	0.081
NEA	14.09	7.27	17.92	21.32	—	0.087	0.115	0.109	0.094	0.083	0.105	0.093	0.109	**0.072**	0.100	0.107
EAM	45.95	27.84	38.52	15.84	38.78	—	0.050	0.049	0.034	0.044	0.047	0.045	0.048	**0.048**	0.042	0.047
AND	130.42	88.48	103.64	63.03	97.27	21.81	—	0.027	0.041	0.057	0.041	0.048	0.041	**0.068**	0.042	0.025
AS	125.02	85.80	102.24	58.70	92.76	23.66	6.80	—	0.035	0.047	0.036	0.032	0.036	**0.062**	0.033	0.019
OCE	83.75	50.61	73.07	38.08	70.04	10.06	10.27	9.87	—	0.035	0.028	0.030	0.032	**0.048**	0.026	0.035
EUP	73.04	37.65	66.66	19.07	52.91	9.03	13.06	8.62	3.03	—	0.039	0.033	0.042	**0.045**	0.033	0.046
AFR	120.94	75.76	102.26	55.10	95.93	24.94	7.65	11.63	8.22	5.11	—	0.034	0.027	**0.059**	0.025	0.034
NW	124.50	74.34	99.50	57.53	92.07	23.93	15.93	6.05	12.55	10.27	14.22	—	0.040	**0.050**	0.029	0.036
KH	100.67	64.11	93.17	34.69	87.54	19.54	17.17	16.70	10.22	3.37	8.37	20.95	—	**0.063**	0.025	0.032
UC	68.22	31.98	49.67	19.75	40.91	3.50	19.85	18.26	10.53	4.12	19.98	13.11	20.86	—	**0.051**	0.062
LUP	95.37	60.89	89.98	37.44	74.53	13.32	8.81	6.65	4.12	0.04	4.94	7.74	5.85	7.11	—	0.032
WE	104.50	62.99	83.61	49.38	76.95	16.92	7.29	4.52	8.39	5.46	10.63	13.63	12.18	18.77	6.66	—

B

|	MPA	MPE	LPA	NEA	EAM	AND	AS	OCE	EUP	AFR	KH	NW	UC	LUP	WE
MPA	—	0.064	0.099	0.066	0.109	0.110	0.107	0.099	0.118	0.107	0.105	0.113	**0.090**	0.105	0.099
MPE	0.00	—	0.107	0.074	0.108	0.111	0.110	0.114	0.114	0.116	0.109	0.122	**0.102**	0.104	0.111
LPA	8.39	18.36	—	0.109	0.106	0.091	0.097	0.077	0.095	0.088	0.087	0.108	**0.090**	0.085	0.096
NEA	0.40	9.38	19.44	—	0.106	0.091	0.097	0.077	0.095	0.088	0.087	0.108	**0.090**	0.085	0.096
EAM	22.17	33.29	27.13	30.26	—	0.116	0.120	0.115	0.107	0.118	0.111	0.134	**0.116**	0.115	0.128
AND	61.23	75.36	21.00	78.27	70.18	—	0.046	0.058	0.069	0.046	0.053	0.061	**0.070**	0.062	0.057
AS	60.06	73.27	17.94	77.65	68.05	5.32	—	0.069	0.074	0.050	0.059	0.030	**0.061**	0.064	0.052
OCE	41.09	65.17	6.27	61.46	54.28	13.85	17.07	—	0.076	0.050	0.059	0.082	**0.050**	0.057	0.062
EUP	35.73	42.43	0.00	46.50	26.30	0.00	0.00	0.98	—	0.074	0.074	0.089	**0.074**	0.066	0.084
AFR	55.35	77.11	16.12	75.96	69.81	8.41	6.61	10.49	6.75	—	0.035	0.061	**0.060**	0.050	0.049
KH	45.00	62.47	13.20	62.81	55.28	15.87	9.97	16.64	6.59	5.68	—	0.075	**0.062**	0.047	0.055
NW	70.79	89.39	25.21	87.11	80.04	9.20	3.22	23.60	8.62	7.37	15.43	—	**0.072**	0.079	0.056
UC	21.28	38.41	0.00	39.89	39.73	12.13	6.01	0.37	0.00	5.66	3.37	14.14	—	**0.052**	0.057
LUP	38.73	48.72	10.11	49.20	51.04	17.42	14.25	15.22	0.00	12.84	10.37	23.09	**0.00**	—	0.062
WE	46.92	65.82	15.55	56.79	69.32	12.52	10.03	17.70	6.30	9.82	9.85	10.75	**4.03**	10.40	—
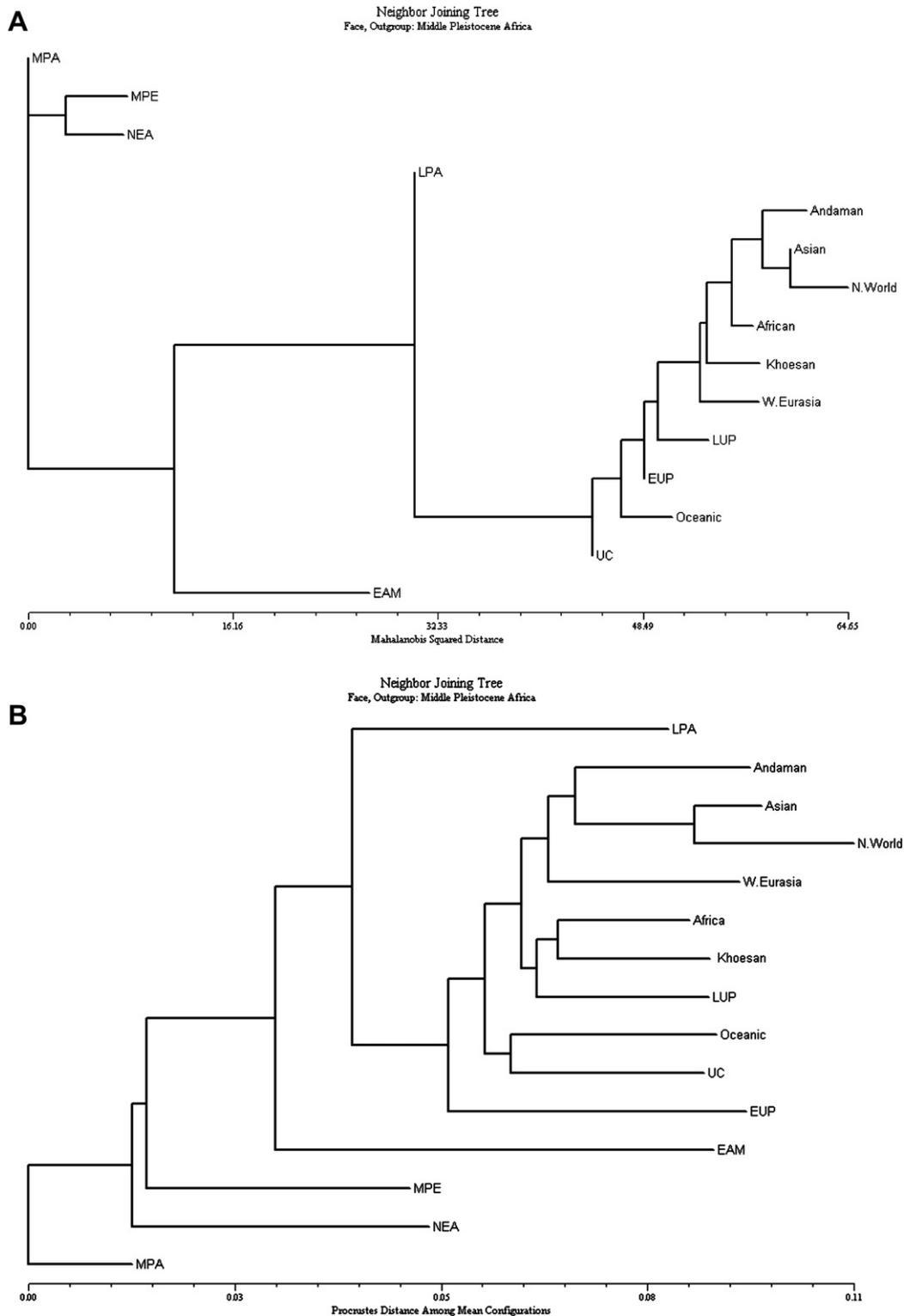
Fig. 4. Neighbor Joining Tree, face dataset. A: Mahalanobis squared distances; B: Procrustes distances among mean sample. Labels are the same as in Tables 1 and 2.

Předmostí 3, while UC 103 was nearest to Mladeč 1 in the shape of its face. Similarities between these specimens have been noticed before (see Stringer and Andrews, 1988: Fig. 1), but the close relationship reported here has not been demonstrated until now. It is interesting to note that, in their recent publication of the early modern human remains from Tianyan cave, Zhoukoudian, Shang et al. (2007) reported a close resemblance in the dental morphology of this specimen with that of Upper Paleolithic specimens from Arene Candide, Dolní Věstonice, and Mladeč, a result very similar to the one reported here. These features and other "archaic"-like traits described by Shang et al. (2007) for Tianyan might also be interpreted as retentions of ancestral modern human morphology, rather than the result of admixture with local archaic populations.

The present analyses also fail to reveal strong affinities between the UC specimens and any of the recent human samples measured. Most importantly, East Asian samples and the Upper Cave material do not appear to be particularly similar, though slight resemblances seem to occur between UC 101 and the Oceanic sample on the one hand, and UC 103 and the New World sample on the other. Furthermore, in the face mean Procrustes Neighbor Joining Tree analysis, the UC sample clusters loosely with the recent Oceanic population. These results are similar to those of previous studies (e.g., Howells, 1983; Habgood, 1986; Kamminga and Wright, 1988; Stringer, 1992a). Because this study does not include either early Australian or American material, it is not possible to explore the links between these early groups and the Upper Cave individuals proposed by some researchers (e.g., Habgood, 1986; Stringer, 1992a; Hanihara, 1994; Neves and Pucciarelli, 1998; Cunningham and Jantz, 2003). However, such a similarity would be consistent with the present results if both UC and early Australians/Americans retained ancestral modern human conditions for aspects of their cranial morphology (see also Schillaci, 2008).

The Upper Cave specimens also do not show particular resemblances to archaic human fossils, including the only archaic East Asian specimen that it was possible to include in the analysis, Dali (only included in the vault dataset because its facial morphology is not fully preserved). Although the combined UC sample is closer in Mahalanobis D^2 to Dali than it is to the African and European Middle Pleistocene samples or to *H. neanderthalensis*, UC is much closer to the Late Pleistocene African, Skhul/Qafzeh, and Upper Paleolithic European material (Table 6). Dali, on the other hand, is nearest neighbor to the Middle Pleistocene specimens from Africa and Europe, Neanderthals, as well as the Late Pleistocene African sample, as also shown in the Neighbor Joining Trees. In terms of inter-individual Procrustes distances, Dali is closest neighbor to Kabwe, Saldanha, and La Ferrassie 1 in the shape of its vault. These results agree broadly with those of Stringer (1992b), who found Dali to be most similar to African and European Middle Pleistocene specimens, and not linked with the UC individuals, as has been proposed by other researchers (Thorne and Wolpoff, 1992).

The present analysis cannot evaluate the recent proposal that the Levantine early modern human population, represented by the Skhul and Qafzeh material, was ancestral to recent Australians to the exclusion of later Eurasian populations, presumably originating from a later Out of Africa expansion ca. 60–40 ka. It does not incorporate early Australians, the group that has been argued to show closest affinities with early modern humans from the Levant (Schillaci, 2008). The recent Oceanic sample in the present study is closer than any other recent human group to either the LPA or the Levantine early modern humans. However, it is even more similar to Upper Paleolithic Europeans, suggesting a possible retention of ancestral morphology in this geographic region (see Lahr, 1996). A recent study (Gunz et al., 2009) has further argued for a high level of variability in the early anatomically modern human sample (represented here by Qafzeh-Skhul as well as the LPA material), and for multiple contributions from these early modern humans to the ancestry of recent human populations. The present analysis also finds the LPA and EAM samples to be quite variable, as would be expected given their wide geographic and temporal range. However, several specimens are found here to be closest neighbors to each other in terms of overall shape (Procrustes distance), suggesting again a certain level of similarity among the specimens included in these geographically and temporally disparate samples. Unlike the findings of Gunz et al. (2009), these specimens are not most similar to extant modern humans in the present analysis–in fact, they are quite distant from all recent human samples in the Mahalanobis D^2 and mean Procrustes distances, and are placed as outgroups to the modern human cluster in all Neighbor Joining

Trees. Furthermore, they are closest neighbors in shape (inter-individual Procrustes distances) in equal degrees to extant modern human individuals, other LPA–EAM specimens, and archaic (including Neanderthal) specimens. Therefore, the argument of a direct phylogenetic contribution of early anatomically modern humans to any particular modern human group cannot be made convincingly based on the present results. Rather, these specimens appear intermediate in their morphology between archaic Middle Pleistocene specimens and extant humans, and closest in overall distances to each other and to Upper Paleolithic samples.

Finally, the high level of morphological heterogeneity in the UC sample is often discussed, and has been interpreted as indicating a higher level of variation in Pleistocene modern human groups compared to recent populations. The inter-individual variability represented in the UC sample was assessed here for UC 101 and UC 103 using Procrustes distances among male and female individuals from each recent human reference sample. This analysis showed that the two specimens differ most in their vault morphology, since their vault Procrustes distance is elevated relative to the mean values for modern human groups. UC 101 and 103 are more similar in their facial morphologies, and their facial Procrustes distance is more comparable to mean values of recent reference samples. The only instance where the UC 101–103 Procrustes distance falls (just) beyond the 95th percentile, but still within the range of a recent sample, is in the vault analysis when it is compared to the extremely homogeneous isolated island Andamanese population. This result supports recent research (Cunningham and Wescott, 2002) showing that the UC individuals probably did not derive from the same family group, as originally suggested (Weidenreich, 1938–39). However, it does indicate that these two individuals, though quite distinct from each other, nonetheless could have been drawn from the same regional, and even the same local, population.

It is worth pointing out in this context that the two datasets used here (neurocranial and facial) might not reflect population history equally. Although the validity of using cranial morphology in phylogenetic analyses has been questioned (see Collard and Wood, 2000), several recent studies have found overall cranial morphology to track population history quite well in modern human populations (e.g., Relethford, 1994, 2004a, b; Roseman, 2004; Harvati and Weaver, 2006a, b; Smith, 2009; Harvati et al., 2009; von Cramon-Taubadel, 2009; Hubbe et al., 2009). The question of whether or not different anatomical regions are better suited for such analysis, however, is still under discussion. Several recent studies have found neurocranial morphology, measured by both 3-D landmark data and conventional linear measurements, to be relatively highly correlated with population history (inferred from either neutral genetic data or using geographic distances as a proxy; Roseman, 2004; Harvati and Weaver, 2006a, b; Harvati et al., 2009; Hubbe et al., 2009). The usefulness of the face in reconstructing phylogeny and population history has often been questioned in the past, as this anatomical region is generally thought to be highly plastic and to be affected by masticatory processes and climate (e.g., Skelton and McHenry, 1992; Wood and Lieberman, 2001; Strand-Viðarsdóttir et al., 2002; Lieberman et al., 2004; Lieberman, 2008). Recent work testing this hypothesis has shown somewhat contradictory results. Harvati and Weaver (2006b) found a climatic, but not a population history, signal in facial morphology using a 3-D geometric morphometric analysis of a sample of 13 modern human populations. However, Smith (2009) found a significant correlation between facial morphology and neutral genetic distances using similar data in her sample of 14 groups. Harvati et al. (2009) and Hubbe et al. (2009) analyzed a very large craniometric dataset (>7000 specimens from 135 populations around the globe) and found a significant correlation between facial measurements and geographic distances (used as a proxy for

population history). In this case, facial measurements also showed a strong climatic signal, restricted to very high-latitude groups. Finally, some aspects of the face, the mandible (Smith, 2009), and the maxilla and zygomatic bone (von Cramon-Taubadel, 2009) have been found to be unreliable for population history reconstruction.

It is therefore likely that the facial analysis of the Upper Cave specimens reflects a combination of population history and environmental factors, perhaps to a greater extent than the neurocranial analysis, which seems likely to preserve a stronger population history signal. Nonetheless, the results of both analyses are remarkably consistent, and, taken together, suggest a close link with Upper Paleolithic European samples and possibly other early modern humans. The present results therefore support the hypothesis that the Upper Cave specimens retain important aspects of morphology that were ancestral to modern humans, and suggest that the UC material may represent members of an as yet undifferentiated early modern human population that expanded across Eurasia in the Late Pleistocene (see Lahr, 1995). They concur with research indicating a degree of morphological homogeneity among European, Asian, and African Late Paleolithic modern human fossils, consistent with the predictions of the Single origin, rather than the Regional Continuity, model for the evolution of modern humans (e.g., Stringer and Andrews, 1988; Bräuer, 1992a, b; Stringer, 1992b, 2002; Grine et al., 2007; Harvati et al., 2007).

Conclusions

The present analysis supports the hypothesis that the Upper Cave specimens retain important aspects of morphology that were ancestral to all modern humans, and that they represent members of an as yet undifferentiated early modern human population that expanded across Eurasia in the Late Pleistocene (see Lahr, 1995). This analysis concurs with research indicating morphological similarity among European, Asian, and African Late Paleolithic modern human fossils, consistent with the predictions of the Single Origin model for the evolution of modern humans (e.g., Stringer and Andrews, 1988; Bräuer, 1992a, b; Stringer, 1992b, 2002; Grine et al., 2007; Harvati et al., 2007). The resolution of the specimens' geological age would help elucidate this matter further. However, if cranial morphometric evidence is indicative of population history, as has been suggested recently (Roseman, 2004; Harvati and Weaver, 2006a, b), these results support a recent common origin for these early modern populations, possibly in the form of a recently shared ancestral group expanding out of Africa in the Late Pleistocene.

Acknowledgments

References

Applied Biostatistics Inc., 1986–2000. NTSYSpc, Version 2.10t. Applied Biostatistics Inc.

Bookstein, F.L., 1997. Landmark methods for forms without landmarks: morphometrics of group differences in outline shape. Med. Image Anal. 1 (3), 225–243.

Bräuer, G., 1989. The Evolution of Modern Humans. In: Mellars, P., Stringer, C. (Eds.), The Human Revolution. A comparison of the African and Non-African Evidence. Princeton University Press, Princeton, pp. 124–154.

Bräuer, G., 1992a. Origins of modern humans. In: Akazawa, T., Aoki, K., Kimoura, T. (Eds.), The Evolution and Dispersal of Modern Humans in Asia. Regional evolution or replacement?. Hokusen-sha, Tokyo, pp. 401–413.

Bräuer, G., 1992b. Africa's place in the evolution of *Homo sapiens*. In: Bräuer, G., Smith, F.H. (Eds.), Continuity or Replacement. Controversies in *Homo sapiens* evolution. A.A. Balkema, Rotterdam, pp. 83–98.

Bräuer, G., Mbua, E., 1992. *Homo erectus* features used in cladistic analysis and their variability in Asian and African hominids. J. Hum. Evol. 22, 79–108.

Brown, P., 1993. Recent human evolution in East Asia and Australasia. Philos. Trans. R. Soc. Lond., B, Biol. Sci. 337, 235–242.

Brown, P., 1998. The first Mongoloids? Another look at Upper Cave 101, Liujiang and Minatogawa 1. Acta Anthropologica Sinica. 17, 255–275.

Brown, P., 1999. The first modern East Asians? Another look at Upper Cave 101, Liujiang and Minatogawa 1. In: Omoto, K. (Ed.), Interdisciplinary Perspectives on the Origins of the Japanese. International Research Center for Japanese Studies, Kyoto, pp. 105–124.

Chen, T., Hedges, R.E.M., Yuan, Z., 1989. Accelerator radiocarbon dating for the Upper Cave of Zhoukoudian. Acta Anthropologica Sinica 8, 216–221.

Collard, M., Wood, B., 2000. How reliable are human phylogenetic hypotheses? Proc. Natl. Acad. Sci. U.S.A. 97, 5003–5006.

Coon, C.S., 1962. The Origin of Races. Knopf, New York.

Cunningham, D.L., Jantz, R.L., 2003. The morphometric relationship of Upper Cave 101 and 103 to modern *Homo sapiens*. J. Hum. Evol. 45, 1–18.

Cunningham, D.L., Wescott, D.J., 2002. Within-group human variation in the Asian Pleistocene: the three Upper Cave crania. J. Hum. Evol. 42, 627–638.

von Cramon-Taubadel, N., 2009. Congruence of individual cranial bone morphology and neutral molecular affinity patterns in modern humans. Am. J. Phys. Anthropol., 140, 205–215.

González-José, R., Bortolini, M.C., Santos, F.R., Bonatto, S.L., 2008. The peopling of America: Craniofacial shape variation on a continental scale and its interpretation from an interdisciplinary view. Am. J. Phys. Anthropol 137, 175–187.

Grine, F.E., Bailey, R.M., Harvati, K., Nathan, R.P., Morris, A.G., Henderson, G.M., Ribot, I., Pike, A.W.G., 2007. Late Pleistocene Human Skull from Hofmeyr, South Africa and Modern Human Origins. Science 315, 226–229.

Groves, C.P., 1989. A regional approach to the problem of the origin of modern humans in Australasia. In: Mellars, P., Stringer, C.B. (Eds.), The Human Revolution. Princeton University Press, Princeton, pp. 274–285.

Gunz, P., 2005. Statistical and geometric reconstruction of hominid crania: Reconstructing australopithecine ontogeny. Ph.D. Dissertation. University of Vienna.

Gunz, P., Harvati, K., 2007. The Neanderthal "chignon": Variation, integration and homology. J. Hum. Evol. 52, 262–274.

Gunz, P., Bookstein, F.L., Mitteroecker, P., Stadlmayr, A., Seidler, H., Weber, G.W., 2009. Early modern human diversity suggests subdivided population structure and a complex out-of-Africa scenario. Proc. Natl. Acad. Sci. U.S.A. 105, 6094–6098.

Gunz, P., Mitteroecker, P., Neubauer, S., Weber, G.W., Bookstein, F.L., 2009. Principles for the Virtual Reconstruction of hominin crania. J. Hum. Evol. 57, 48–62.

Habgood, P.J., 1986. The origin of the Australian aborigines: A multivariate approach and view. Archaeology in Oceania 21, 130–137.

Habgood, P.J., 1989. The origin of anatomically modern humans in Australasia. In: Mellars, P., Stringer, C.B. (Eds.), The Human Revolution. Princeton University Press, Princeton, pp. 245–273.

Hanihara, T., 1994. Craniofacial continuity and discontinuity of Far Easterners in the Late Pleistocene and Holocene. J. Hum. Evol. 27, 417–441.

Harvati, K., 2003. Quantitative analysis of Neanderthal temporal bone morphology using 3-D geometric morphometrics. Am. J. Phys. Anthropol. 120, 323–338.

Harvati, K., Weaver, T.D., 2006a. Reliability of cranial morphology in reconstructing Neanderthal phylogeny. In: Harvati, K., Harrison, T. (Eds.), Neanderthals Revisited. New Approaches and Perspectives. Springer, Dordrecht, pp. 239–254.

Harvati, K., Weaver, T.D., 2006b. Human cranial anatomy and the differential preservation of population history and climate signatures. Anat. Rec. 288A, 1225–1233.

Harvati, K., Frost, S.R., McNulty, K.P., 2005. Neanderthal variation and taxonomy – A reply to Ackermann (2005) and Ahern et al. (2005). J. Hum. Evol. 48, 653–660.

Harvati, K., Gunz, P., Grigorescu, D., 2007. Cioclovina (Romania): Morphological affinities of an early modern European. J. Hum. Evol. 53, 732–746.

Harvati, K., Hubbe, M., Bernardo, D.V., Hanihara, T., 2009. Population history and cranial morphology in a large human skeletal dataset. Am. J. Phys. Anthropol. S48, 145–146.

Hedges, R.E.M., Housley, R.A., Bronk, C.R., Van Klinken, G.J., 1992. Radiocarbon dates from the Oxford AMS system: Archaeometry Datelist 14. Archaeometry 34, 141–159.

Howells, W.W., 1983. Origins of the Chinese people: Interpretations of the recent evidence. In: Keightley, D. (Ed.), The Origins of Chinese Civilization. University of California Press, Berkeley, pp. 297–319.

Howells, W.W., 1989. Skull Shapes and the Map: Craniometric Analyses in the Dispersion of Modern Homo. In: Papers of the Peabody Museum of Archaeology and Ethnology, vol. 79. Harvard University.

Howells, W.W., 1992. Getting Here: The Story of Human Evolution. The Compass Press, Washington, D.C.

Hubbe, M., Hanihara, T., Harvati, K., 2009. Climate signatures in the morphological differentiation of world-wide modern human populations. Anat. Rec. in press., doi:10.1002/ar.20976.

Immersion Corp., 1998. Microscribe 3D User's Guide. Immersion Corporation, San Jose, CA.

Kamminga, J., 1992. New interpretations of the Upper Cave, Zhoukoudian. In: Akazawa, T., Aoki, K., Kimoura, T. (Eds.), The Evolution and Dispersal of Modern Humans in Asia. Hokusen-sha, Tokyo, pp. 379–400.

Kamminga, J., Wright, R.V.S., 1988. The Upper Cave at Zhoukoudian and the origin of the Mongoloids. J. Hum. Evol. 17, 739–767.

Kaiser, H.F., 1961. A note on Guttman's lower bound for the number of common factors. Brit. J. Psychol. 14, 1–2.

Lahr, M., 1994. The multiregional model of modern human origins: A reassessment of its morphological basis. J. Hum. Evol. 26, 23–56.

Lahr, M., 1995. Patterns of modern human diversification: Implications for Amerindian origins. Yearb. Phys. Anthropol. 38, 163–198.

Lahr, M.M., 1996. The Evolution of Modern Human Diversity: A Study of Cranial Variation. Cambridge Press, Cambridge.

Lieberman, D.E., 1995. Testing hypotheses about recent human evolution from skulls: Integrating morphology, function, development, and phylogeny. Curr. Anthropol 36, 159–197.

Lieberman, D.E., 2008. Speculations about the selective basis for modern human craniofacial form. Evol. Anthropol. 17, 55–68.

Lieberman, D.E., Krovitz, G.E., Yates, F.W., Devlin, M., St. Claire, M., 2004. Effects of food processing on masticatory strain and craniofacial growth in a retrognathic face. J. Hum. Evol. 46, 655–677.

Liu, W., Vialet, A., Wu, X., He, J., Lu, J., 2006. Comparaison de l'expression de certains caractères crâniens sur les hominidés chinois du Pléistocène récent et de l'Holocène (grotte supérieure de Zhoukoudian, sites de Longxian et de Yanqing). Anthropologie 110, 258–276.

Marcus, L.F., 1993. Some aspects of multivariate statistics for morphometrics. In: Marcus, L.F., Bello, E., García-Valdecasas, A. (Eds.), Contributions to Morphometrics. Monografias Museo Nacional de Ciencias Naturales, Madrid, pp. 99–130.

Mardia, K.V., Bookstein, F.L., 2000. Statistical assessment of bilateral symmetry of shapes. Biometrika 87, 285–300.

McNulty, K.P., Smith, H., 2009. Data were collected from high-quality casts. "Abstracts of the PaleoAnthropology Society 2009 Meetings". PaleoAnthropology 2009, A25.

Neves, W., Pucciarelli, H., 1998. The Zhoukoudian Upper Cave skull 101 as seen from the Americas. J. Hum. Evol. 34, 219–222.

O'Higgins, P., 2000. The study of morphological variation in the hominid fossil record: Biology, landmarks and geometry. J. Anat. 197, 103–120.

Relethford, J.H., 1994. Craniometric variation among modern human populations. Am. J. Phys. Anthropol. 95, 53–62.

Relethford, J.H., 2004a. Boas and beyond: Migration and craniometric variation. Am. J. Hum. Biol. 16, 379–386.

Relethford, J.H., 2004b. Global patterns of isolation by distance based on genetic and morphological data. Hum. Biol. 76, 499–513.

Rohlf, F.J., 2003. tpsSmall v. 1.20. Department of Ecology and Evolution, State University of New York, Stony Brook, New York.

Rohlf, F.J., Marcus, L.F., 1993. A revolution in morphometrics. Trends Ecol. Evol. 8, 129–132.

Roseman, C.C., 2004. Detection of interregionally diversifying natural selection on modern human cranial form by using matched molecular and morphometric data. Proc. Natl. Acad. Sci. U.S.A. 101, 12824–12829.

SAS Institute, 1999–2001. SAS System for Windows V8. The SAS Institute.

Schillaci, M.A., 2008. Human cranial diversity and evidence for an ancient lineage of modern humans. J. Hum. Evol. 54, 814–826.

Shang, H., Tong, H., Zhang, S., Chen, F., Trinkaus, E.T., 2007. An early modern human from Tianyuan Cave, Zhoukoudian, China. Proc. Natl. Acad. Sci. U.S.A. 104, 6573–6578.

Skelton, R.R., McHenry, H.M., 1992. Evolutionary relationships among early hominids. J. Hum. Evol. 23, 309–349.

Slice, D.E., 1998. Morpheus et al.: software for morphometric research. Revision 01–30–98. Department of Ecology and Evolution, State University of New York, Stony Brook, New York.

Smith, H.S., 2009. Which Cranial Regions Reflect Molecular Distances Reliably in Humans? Evidence from Three-Dimensional Morphology. Am. J. Hum. Biol. 21, 36–47.

Strand-Viðarsdóttir, U., O'Higgins, P., Stringer, C., 2002. A geometric morphometric study of regional differences in the ontogeny of the modern human facial skeleton. J. Anat. 201, 211–229.

Stringer, C.B., 1992a. Reconstructing recent human evolution. Philos. Trans. R. Soc. Lond., B, Biol. Sci. 337, 217–224.

Stringer, C.B., 1992b. Replacement, continuity and the origin of Homo sapiens. In: Bräuer, G., Smith, F.H. (Eds.), Continuity or Replacement. Controversies in Homo sapiens evolution. A.A. Balkema, Rotterdam, pp. 9–24.

Stringer, C.B., 2002. Modern human origins: progress and prospects. Philos. Trans. R. Soc. Lond., B, Biol. Sci. 357, 563–579.

Stringer, C.B., Andrews, P., 1988. Genetic and fossil evidence for the origin of modern humans. Science 239, 1263–1268.

Stynder, D.D., Ackermann, R.R., Sealy, J.C., 2007. Craniofacial variation and population continuity during the South African Holocene. Am. J. Phys. Anthropol. 134, 489–500.

Thorne, A.E., Wolpoff, M.H., 1992. The multiregional evolution of humans. Sci. Am. 266, 28–33.

Trinkaus, E.T., 2005. Early modern humans. Ann. Rev. Anthropol. 34, 207–230.

Turner II, C.G., 1985. The dental search for Native American origins. In: Kirk, R., Szathmary, E. (Eds.), Out of Asia. Peopling the Americas and the Pacific. Australian National University, Canberra.

Turner II, C.G., Manabe, Y., Hawkey, D.E., 2000. The Zhoukoudian Upper Cave dentition. Acta Anthropol. Sin. 19, 253–268.

Weidenreich, F., 1938–39. On the earliest representatives of modern mankind recovered on the soil of East Asia. Pek. Nat. Hist. Bul. 13, 161–174.

Wolfram Research, Inc., 2007. Mathematica Edition, Version 6.0. Wolfram Research, Inc., Champaign, Illinois.

Wolpoff, M.H., 1995. Wright for the wrong reasons. J. Hum. Evol. 29, 185–188.

Wolpoff, M.H., 1996. Human Evolution, 1996-1997 Edition. McGraw-Hill, New York.

Wood, B., Lieberman, D.E., 2001. Craniodental variation in Paranthropus boisei: A developmental and functional perspective. Am. J. Phys. Anthropol 116, 13–25.

Wright, R.V.S., 1992. Correlation between cranial form and geography in Homo sapiens: CRANID–a computer program for forensic and other applications. Arch. Oceania 27, 128–134.

Wright, R.V.S., 1995. The Zhoukoudian Upper Cave skull 101 and multiregionalism. J. Hum. Evol. 29, 181–183.

Wu, X., 1960. On the racial types of the Upper Cave Man of Choukoudian. Sci. Sin. 10, 998–1006.

Wu, X., 1961. Study on the Upper Cave man of Choukoutien. Vert. Palasiatica 5, 181–211.

Wu, X., Wang, L., 1985. Chronology in Chinese Palaeoanthropology. In: Wu, R., Olsen, J.W. (Eds.), Palaeoanthropology and Palaeolithic Archaeology in the People's Republic of China. Academic Press, London, pp. 29–68.